Naval Research Laboratory
Washington, DC 20375-5000

NRL Memorandum Report 6376

A Method for Approximating the Initial Data Plane for Surface Ship Wake Simulations

E. WADE MINER

Center for Hydrodynamic Development
Laboratory for Computational Physics and Fluid Dynamics

STEVEN E. RAMBERG

Ocean Technology Program
Office of Naval Research

THOMAS F. SWEAN, JR.

Center for Hydrodynamic Development
Laboratory for Computational Physics and Fluid Dynamics

November 30, 1988

SECURITY CLASSIFICATION OF THIS PAGE

AD-A202 423

REPORT DOCUMENTATION PAGE

Form Approved OMB No 0704-0188

1a. REPORT SECURITY CLASSIFICATION UNCLASSIFIED	1b RESTRICTIVE MARKINGS
2a. SECURITY CLASSIFICATION AUTHORITY	3 DISTRIBUTION/AVAILABILITY OF REPORT Approved for public release; distribution unlimited.
2b. DECLASSIFICATION/DOWNGRADING SCHEDULE	
4. PERFORMING ORGANIZATION REPORT NUMBER(S) NRL Memorandum Report 6376	5 MONITORING ORGANIZATION REPORT NUMBER(S)
6a. NAME OF PERFORMING ORGANIZATION Naval Research Laboratory 6b. OFFICE SYMBOL (If applicable) Code 4430	7a. NAME OF MONITORING ORGANIZATION
6c. ADDRESS (City, State, and ZIP Code) Washington, DC 20375-5000	7b ADDRESS (City, State, and ZIP Code)
8a. NAME OF FUNDING/SPONSORING ORGANIZATION Office of Naval Research 8b OFFICE SYMBOL (If applicable)	9 PROCUREMENT INSTRUMENT IDENTIFICATION NUMBER
8c. ADDRESS (City, State, and ZIP Code) Arlington, VA 22217	10 SOURCE OF FUNDING NUMBERS PROGRAM ELEMENT NO: 61153N; PROJECT NO:; TASK NO: RR023-01-00; WORK UNIT ACCESSION NO:

11. TITLE (Include Security Classification)

A Method for Approximating the Initial Data Plane for Surface Ship Wake Simulations

12. PERSONAL AUTHOR(S)

Miner, E. Wade, Ramberg, Steven E. and Swean, Thomas F., Jr.

13a. TYPE OF REPORT	13b TIME COVERED	14 DATE OF REPORT (Year, Month, Day)	15 PAGE COUNT
Interim	FROM 8/87 TO present	1988 November 30	44

16. SUPPLEMENTARY NOTATION

*Ocean Technology Program, Office of Naval Research

17. COSATI CODES		
FIELD	GROUP	SUB-GROUP

18 SUBJECT TERMS (Continue on reverse if necessary and identify by block number)

Surface ship wake; Initial data plane. (cdc)
Parabolic Navier-Stokes equations;
Numerical simulations; Self-propelled wake

19. ABSTRACT (Continue on reverse if necessary and identify by block number)

A procedure for obtaining a set of nearwake iniital condition data for the parabolic numerical simulation of the turbulent far wake of a surface ship is developed. The principal elements of a surface ship wake are considered and are modeled based on experimental data. The wakes of the individual elements are assembled using linear superposition. Interactions among elements are discussed but not modelled. The superposition procedure is implemented in a computer code which uses parameters of the ship as program input. Results generated by the code for a guided missile destroyer model are presented and compared with limited experimental data. Keywords:

20. DISTRIBUTION/AVAILABILITY OF ABSTRACT	21 ABSTRACT SECURITY CLASSIFICATION
☒ UNCLASSIFIED/UNLIMITED ☐ SAME AS RPT ☐ DTIC USERS	UNCLASSIFIED
22a. NAME OF RESPONSIBLE INDIVIDUAL E. Wade Miner	22b TELEPHONE (Include Area Code) (202) 767-3389 22c OFFICE SYMBOL Code 4430

DD Form 1473, JUN 86 Previous editions are obsolete SECURITY CLASSIFICATION OF THIS PAGE

S/N 0102-LF-014-6603

CONTENTS

A METHOD FOR APPROXIMATING THE INITIAL DATA PLANE FOR SURFACE SHIP WAKE SIMULATIONS

1. INTRODUCTION

For some time, remotely sensed data of the ocean surface have been used to determine surface conditions, such as wave height and wind direction. From the outset it was clear that ship wake features could be readily identified in the remotely sensed data (e.g. SEASAT-A). The recent SIR/B series of synthetic aperture radar (SAR) experiments were analyzed by Hawkins, et al. (1986) and clearly showed that surface vessels can be located by wake detection and that it may be possible to classify ship types by certain wake characteristics. As a result of these and other observations, the hydrodynamic characteristics of surface ship wakes have been of growing interest. One major component of a ship wake which is often imaged is the turbulent wake region along the ship track. In a SAR image it usually appears brighter than ambient directly behind the ship before decaying to a long linear dark feature marking the ship's course. In a visual image such as the Scully-Power (1986) space shuttle photograph the track signature can be bright or dark depending on the relative locations of the observer, the target and the sun's illumination. The signatures are presumably due to changes in the ambient surface roughness at the wavelengths appropriate to the sensor system(s) arising from the passage of a ship. Milgram (1988) examines the radar backscatter from short diverging waves in the wake of a ship and finds that these waves are consistent with the bright V patterns found in many SAR images. Milgram concludes that the flow field around and behind the ship is expected to significantly affect the observed images. A full explanation of the signatures observed by various sensor systems will require modelling of the turbulent wake of the surface ship and its interactions with ambient and other wake processes which modulate the surface roughness. When such an explanation is available it may be used to locate and identify ships at sea for surveilance purposes and/or it may be used to determine local environmental conditions. Information of this sort can be used directly or as input to other military or commercial considerations.

The state of the art in computational fluid mechanics has reached a point where it is practical to numerically simulate the development of the far wake of a surface vessel via "parabolized" Navier-Stokes numerical methods. Examples of such codes are the

Manuscript approved October 6, 1988.

3DPNS code of Baker (1982) and the SURFWAKE code of Meng (1985). Such codes require an initial plane of data which is marched downstream to obtain the solution in the far wake. The parabolic approach is taken to reduce computational needs that would arise with the use of more general elliptic or partially-parabolic methods. The quality and validity of any parabolic solution ultimately depends on the quality and validity of the initial plane data for mean flow and turbulence quantities.

It is possible to completely initialize the wake simulation with data obtained experimentally from the wake of a full scale or a model vessel. Unfortunately, such data sets are not available except in part and then for only a few ship configurations at model scale. Moreover, detailed experimental data would not be available for use in a design process where a requirement might be to minimize one or more wake features.

An alternative to using experimental data for initializing a far wake simulation is to use results obtained from a calculation of the turbulent flow field around the vessel. Landweber and Patel (1979) reviewed the state of the art for calculating ship boundary layers and discussed some of the difficulties involved in such simulations. Boundary layer calculations are dependent upon specification of the surrounding pressure field. For a ship, the imposed pressure field is dependent, in part, upon the surface wave field (ship plus ambient) which interacts with the boundary layer and the ship motions. Thus, the flow field about the ship hull is fully three dimensional, elliptic and unsteady with a free surface. Since Landweber and Patel's review, progress has been made both in computational fluid mechanics and in computer hardware; however, it will still be a number of years before overall computational capabilities reach a point where the calculation of the turbulent flow about a ship hull and in the near wake will be routinely practical without severe restrictions (c.f. Watson - 1987). The necessary data for initializing the numerical simulation of a ship's far wake may be obtained by calculation of the full flow field through the near wake at a high cost in computer resources and time, or by much more economical approximate methods. Often the appropriate choice will be the use of approximate methods. This report describes a method for approximating much of the required initializing data.

The present model for initial condition data follows, in some ways, the works of Meng (1985) and of Hyman (1987). Several features are modified and some features are added. In particular, the hull wake is treated differently and the present model includes the breaking bow wave and includes a variation of Swanson's (1984) bilge vortex model in the set of initial condition data. The models of the wake elements are matched to the major ship parameters and integral constraints on the wake components are implemented in the computer code SURFIN (surface wake initialization). As noted, all

of the wake component models are approximate, therefore, it is to be expected that the model will be refined and improved as more information and data become available.

2. WAKE DESCRIPTION

Most early work on turbulent ship wakes concerned the submerged wakes of submarines. Lin and Pao (1979) have summarized their experimental results for the wakes of axisymmetric submerged bodies upon which much subsequent work has been based. The numerical work of Meng and Innis (1977) was directed toward the simulation of submarine wakes. Submarine wakes are largely composed of axisymmetric elements which tend to be aligned to yield overall axisymmetry for the composite wake as well. More recently, Meng (1985) and Hyman (1987) have considered surface ship wakes and have addressed the problem of determining initial condition data. Ship forms are not axisymmetric and the drag producing elements tend not to be aligned with the thrust elements which also usually occur in pairs not aligned with the direction of travel or with each other. Moreover, the thrust of a surface ship wake exceeds the combined skin friction drag, form drag and resistance augmentation in order to balance the wavemaking resistance of the hull. Due to wave breaking some of the wavemaking resistance may appear as a contribution to the wake mean velocity deficit. Finally, the presence of the free surface and its behavior in the immediate vicinity of the turbulent flow about and behind the hull has no counterpart in normal submarine wakes. These features are considered in the development of the present model.

One of the principal difficulties in specifying initial plane data for surface wakes is the inherent three dimensional and developing character of the flow in the early wake. We will construct the flow field from components which are themselves fully-developed. This implies similarity and generally produces Gaussian distributions for the flow characteristics (c.f. Schlichting – 1968). This simple approach obviously ignores the interactions which will occur during the development of each wake component and precludes initialization in the very near wake. The initial data plane is generally taken to be several beam-widths aft of the ship in order to assure small axial gradients and the appropriateness of the similarity solutions. This limitation is unavoidable at present and may only be removed after considerably more data on the near wakes of ships is available. Very little information is available for three dimensional wake flows. We have drawn somewhat on the literature for three dimensional jet flows (c.f. Rajaratnam – 1976) under the assumption that general differences between two and three dimensional wake flows will parallel differences in jet behavior in two and three dimensions. For example, we assume that slender wakes and jets have similar

transitions to axisymmetric farfield behavior but the transition is longer for wakes than jets owing to lower entrainment and spreading rates.

The principal components contributing to the overall wake of a surface ship are the the hull, rudders, bilge keels, propeller shafts, and supporting struts which produce axial velocity deficits. The propellers produce axial velocities excesses and transverse velocities. For each drag producing element, it is assumed that the frictional drag is the dominant contributor to the velocity defficit. It is expected that the hull has a transom stern and that the form drag of the hull is small. The other elements are expected to be reasonably streamlined and so have low form drag. The operation of the propellers produces a reduction in pressure upstream of the propeller disc. This reduction in pressure on the aft portion of the ship hull has the effect of increasing or augmenting the hull resistance. The present model does not have separate provisions for the form drag and the resistance augmentation. These may be accounted for by increasing the frictional resistance.

While the breaking bow wave is not a part of the ship itself, it is usually present and can contribute significantly to the momentum deficit near the surface and outboard of the hull wake. Trailing vortices from the hull will contribute to the ship wake as will vortices generated by the rudder and bilge keels under certain operating conditions. Multiple bilge vortices have been visualized in ship model tests and their existence verified at full scale as discussed by Hoekstra (1974). The origins of the bilge vortices appear to be three-dimensional flow separation near the bow, along the turn of the bilge and at a transom stern. Swanson (1984) has drawn on an analogy with wingtip trailing vortices to model these structures but this greatly overestimates the vortex strengths and produces only one pair of vortices. Greater similarities are seen with the trailing vortex structure behind delta wings or missles at high angles of attack where three dimensional separation produces steady trailing vortices. In the case of a ship, the secondary flows leading to the trailing vortices stem from the hullform and sinkage and trim of the vessel rather than from lift due to an angle of attack.

3. WAKE COMPONENT MODELS

The following paragraphs describe the models and associated parameters chosen to represent the individual wake components. In most cases, the mean flow of the individual component is integrated to obtain the drag or thrust of that component, and the resulting values are used to select some of the parameters in the model equations. The integral constraints on the components and their assembly are as follows:

1) the total axial momentum deficit of the hull should equal the frictional drag of the bare hull,

2) the rudder and other appendage deficits should yield drags that are appropriate percentages of the bare hull drag,
3) the net propeller thrust should balance the combined hull, appendage and wave drag,
4) the wave drag includes the momentum deficit that may appear in the wake as a result of wave breaking of the bow wave and,
5) the total angular momentum in the propeller jet should match the torque applied by the propeller and this is related to the thrust through the propeller efficiency.

The nomenclature for the model components is based on a ship of length L and beam B travelling with a velocity U_0 in the negative x direction. The y direction is positive down from the free surface, z is the lateral axis that forms a right handed system and the origin is the stern of the ship. The respective mean wake velocities are u, v and w with q as the total turbulent kinetic energy. The ship draft is denoted by D and the propeller diameter by D_p. Other quantities are defined as needed.

3.1 Hull

Most of the experimental data for wakes have been for wakes of towed or self-propelled axisymmetric bodies as in the studies of Pao and Lin (1973a,b), Lin and Pao (1974, 1979), Swanson and Schetz (1974), Gran (1973) and others. A limited number of measurements of the two dimensional wake of submerged flat plates, e.g. Swean (1984), Chevray (1969), are also available. A few studies, e.g. Mitra, Neu and Schetz (1985) and Swean (1984), have considered the effects of the free surface on the wake where a slight migration of the peak mean velocity toward the free surface has been reported. This small, farfield effect is not included here. The axial velocities in the wakes of towed axisymmetric bodies and flat plates are modeled well by Gaussian distributions (Schlichting – 1968). Thus, for the submerged three dimensional wake of a ship hull, we assume the axial mean flow velocity can be represented by the Gaussian profile

$$u_d = u_{d_{max}} e^{-\tilde{a}\left[\left(\frac{y}{y_h}\right)^2+\left(\frac{z}{z_h}\right)^2\right]} \tag{1}$$

where y_h and z_h are the half widths of the wake in the y and z directions. The maximum value of the velocity defect in the wake, $u_{d_{max}}$, is a function of the downstream coordinate x and $\tilde{a}$ is a constant that best fits experimental data. For axisymmetric towed bodies, Pao and Lin (1973) obtained $\tilde{a} = 2.6$. This value has been used for ship wakes as well by Meng (1985), while Hyman (1987) uses 3.0. For bluff jets where the aspect ratio approaches one, a rapid transition to axisymmetric behavior has been

reported within a few characteristic jet dimensions downstream. Slender jets have a longer transition to axisymmetric behavior with the amount depending on the initial aspect ratio and shape (e.g. – rectangular or elliptic). Limited bluff wake measurements by Kuo and Baldwin (1966) indicate a similar behavior. The analagous aspect ratio for a ship hull would be the ship beam divided by twice the draft since the free surface bisects the above profile as a plane of symmetry. This ratio is typically about 1.5 for a variety of ships and exceptions are closer to 1.0. Thus the use of $\tilde{a} = 2.6$ seems warranted by the best available data for axisymmetric wakes.

The integral of the above velocity deficit in the wake yields the frictional drag on the hull which is

$$drag = \frac{\pi}{2\tilde{a}} \rho U_0 u_{d_{max}} y_h z_h \tag{2}$$

when the integration is only over the actual wake, $y \geq 0$. Equation (2) is used in connection with values of the hull drag and of the wake half widths to determine the peak value of u_d and therefore the mean velocity profile due to the hull.

In operation, the present wake model requires values of the frictional resistance of the ship and of the wave resistance of the vessel. The principal contributions to the total ship drag are the frictional resistance and the wave resistance. The contributions to the total drag from resistance augmentation and form drag are usually much smaller in magnitude and so are not explicitly included in the present model. The user may provide the model with values of the frictional and wave resistance, or the model can provide its estimates for the frictional and/or wave resistance. The basis for the resistance estimates follows.

Numerous methods have been used to estimate the frictional drag of the bare hull. The Schoenherr line gives the skin friction coefficient for "clean" turbulent flow and has been used as a lower limit for the hull drag. Several alternate skin friction curves have been proposed and used. Todd (1967) gives a description of several such alternatives. The most widely used curve is probably that adopted by the International Towing Tank Conference at its 1957 meeting in Madrid. This curve is known as the ITTC (1957) curve and is given by the equation

$$C_f = 0.075/\left(\log_{10} Re - 2\right)^2 \tag{3}$$

where Re is the hull Reynolds number and C_f is the skin friction or wetted area drag coefficient. When the input value of frictional ship resistance is zero, the present model

will compute a drag from this relationship which is representative of a smooth, bare flat hull in a turbulent flow.

The estimate for the wave drag in the model is determined in the following manner. Hoerner (1965) notes that the average wave drag (disregarding local resonances where the bow and stern waves reinforce each other or partially cancel each other out) is expected to grow as the 4^{th} power of the Froude Number. For the range of Froude numbers of 0.2 to 0.5, the data which Hoerner gives for destroyers, cruisers and other large naval vessels, appear to fit the following equation well

$$\frac{\text{wave drag}}{\text{displacement}} = (F_r)^4 \tag{4}$$

where displacement is the vessel's weight and $Fr = U_0/\sqrt{gL}$. Below a Froude number of 0.2, Eq. (4) underestimates the wave drag. For $Fr > 0.5$, Eq. (4) overestimates the wave drag. If a zero input value is provided for the wave drag, Eq. (4) provides an estimate for the wave resistance. In the model, the total resistance of the ship is taken as the sum of the values for the frictional resistance and the wave drag.

There are several difficulties involved in estimating y_h and z_h. For two dimensional and axisymmetric jets and wakes the characteristic half widths b will grow as

$$b/b_0 = \tilde{a}(x/b_0 - x_0/b_0)^f \tag{5}$$

where x_0 is a virtual origin which depends on geometry and varies somewhat from one set of experimental conditions to another. The exponent f is $\frac{1}{2}$ for planar and $\frac{1}{3}$ for axisymmetric wakes (see, for example, Schlichting - 1968). Again $\tilde{a}$ is a constant to be selected based on experimental data for the corresponding case. For three dimensional wakes and jets two characteristic wake widths are necessary and two different scales b_0 are available to nondimensionalize the widths. We expand on the method outlined by Hyman (1987) as follows. By analogy with axisymmetric wakes it is assumed that the two wake scales vary individually as

$$y_h = \tilde{a}_y \left[D^2 (x - x_0)\right]^{1/3} \tag{6a}$$

and

$$z_h = \tilde{a}_z \left[(B/2)^2 (x - x_0)\right]^{1/3} \tag{6b}$$

as adapted from Swain (1929) or Blevins (1983). The ratio of scales becomes

$$z_h/y_h = (\tilde{a}_z/\tilde{a}_y)(B/2D)^{2/3} \tag{7}$$

if the same virtual origin is assumed.

Hyman (1987) noted that the data from the MAP WAKE experiments showed that the ratio of z_h to y_h was was six to seven. The data of Lindenmuth (1987) for DTRC model #5415-1 (a high speed destroyer model) indicate a similarly proportioned deficit wake that is perhaps three times the model beam and about one half of the model draft, although some of the lower deficit due to the hull wake may be obscured by the propeller thrust wake. Lindenmuth attributes the extra width of the wake to a breaking bow wave. This is consistent with other wake surveys as discussed by Baba (1969, 1976). The acoustic bubble data from the MAP WAKE system would not differentiate between the bubble wakes of the hull and the breaking bow waves.

Other factors may effect the spreading of the hull wake. The free surface is more than a simple image plane and limits the vertical turbulent wake scales to the lower half plane whereas the horizontal turbulent scales can encompass the entire wake width. In this sense a two-dimensional jet at a free surface behaves more like a wall jet than half of an unbounded jet (Ramberg, Swean and Plesniak - 1988). This does not alter the exponent in Eq. (5) but will reduce the value of $\tilde{a}$ by as much as 30-40 percent and may influence the effective virtual origin x_0 as well. We incorporate this behavior into the model by taking the ratio of $\tilde{a}_z/\tilde{a}_y$ to be 2.0 in Eq. (7).

Many studies, for example Pao and Lin (1973a), show that stratification will inhibit vertical spreading. This may not be significant for typical mixed layer depths at sea but most tow channels have a measurable thermal depth variation which could influence model measurements of wake spreading at larger distances downwake. Stratification would tend to further increase the ratio z_h/y_h in the far wake but the effect is not included here.

In order to obtain one more relation to completely determine the three quantities y_h, z_h and $u_{d_{max}}$ one might assume that the product of the two wake scales will grow as the square of the axisymmetric growth rate. In view of Eq. (2) this is equivalent to the assumption that the maximum velocity decays exactly as in the axisymmetric case. In keeping with the above arguments we have chosen instead to assume that the lateral wake scale varies like the axisymmetric scale or

$$z_h = \tilde{a}_z D\Big(\frac{x - x_0}{D}\Big)^{1/3} + \frac{w_t}{2} \tag{8}$$

where the empirical constants are again from Lin and Pao (1974) and w_t is the width of the ship transom. This assumption is consistent with the bluff wake approximation and will produce a hull wake that decays more slowly.

The turbulent kinetic energy exhibits a double peak which corresponds approximately to the production of turbulence in the boundary layer on each side of the body. Based on the experimental data of Lin and Pao (1973, 1974), both Meng (1985) and Innis (1986) have modeled the turbulence kinetic energy by

$$q = q_{max}\left[\tilde{a}_1 e^{-\tilde{a}_2\left[\left(\frac{y}{y_h}\right)^2+\left(\frac{z}{z_h}\right)^2\right]} - \tilde{a}_3 e^{-\tilde{a}_4\left[\left(\frac{y}{y_h}\right)^2+\left(\frac{z}{z_h}\right)^2\right]}\right] \tag{9}$$

where the peak value of the turbulence kinetic energy is q_{max} and $\tilde{a}_1$, $\tilde{a}_2$, $\tilde{a}_3$ and $\tilde{a}_4$ were chosen to fit the experimental data. Meng chose the following values: 1.35, 1.0, 0.45 and 8.22. These values are also used by Innis and are used in the present model. The values of y_h and z_h are taken to be the same as used in the velocity defect equation. The downstream evolution of q_{max} is uncertain, but is guided by the experimental data of Lin and Pao and others. The data for several cases show that

$$\sqrt{\frac{q_{max}}{u_{d_{max}}^2}} = \begin{cases} 1.45, & \text{for a towed disc;} \\ 0.59, & \text{for a self-propelled slender body;} \\ 0.22, & \text{for a towed slender body.} \end{cases}$$

On the assumption that the propeller contributes significantly to the turbulence kinetic energy of the self-propelled slender body (see, for example, Swean - 1987a), q_{max} for the hull alone is taken to be $\sqrt{q_{max}}/u_{d_{max}} = 0.3$ as an intermediate value. Later the additional turbulence in the propeller jet(s) will be included.

3.2 Appendages

The wakes of individual appendages are modeled similarly to the hull wake with the axial velocity given by Eq. (1) and the turbulence kinetic energy given by Eq. (9) after both are suitably transformed to local coordinates. The input data to the model for the appendages requires the location of the appendage end points. The local z axis is along the major dimension H of the appendage while the y direction is across the appendage width W. For each appendage, the model expects a value for the appendage drag given as a percentage of the hull frictional drag. The model does not provide a default extimate for the appendage drag, and input values of zero give an appendage drag of zero. The user should input to the model values of appendage drag that are

appropriate to the design being considered. In the absence of data from model tests or appendage drag codes, general guidance for the appendage drag as a percentage of the bare hull drag can be obtained from the estimates given by Hoerner (1965):

shaft and struts	7 – 9%
rudders	6 – 7%
bilge keels	1 – 2%.

If the user has access to more appropriate values for the appendage drag, those values should be input. The appendage drag is used with the wake spreading parameters for the appendages, which are discussed below, to determine the value of $u_{d_{max}}$ for the appendages. Equation (2) is used to calculate $u_{d_{max}}$ with the change that the right side of Eq. (2) is multiplied by 2.0, since Eq. (1) is integrated over the full plane for the appendage drag and only over the half plane for the hull drag.

As earlier, we need two more relations to completely determine both wake scales and the maximum velocity. Unlike the hull, most appendages are slender with large aspect ratios H/W. The behavior of jets with such ratios can be described simply as follows (see Rajaratnam – 1976). In the near field (x/W less than 4 to 6) the major wake scale remains constant and may even decrease slightly while the lesser scale grows rapidly in nearly a two-dimensional manner. Within a transition length of a few more W the lesser scale exceeds the major scale and in the far field both scales approach an axisymmetric behavior as they approach one another. The rapid approach to scales of the same order growing at about the same rate is not likely in a slender wake flow in view of the lower entrainment and spreading rates. This difference can be seen in the elliptic wake measurements of Kuo and Baldwin (1966). We assume that the initial data plane is close to the developed region so that the major scale is nearly constant at $z_h = H/2$ and the lesser scale is growing according to

$$y_h = \tilde{a}_a (Wx)^{1/2} + W/2 \tag{10}$$

which is from Blevins (1983) for two dimensional flat plates with $\tilde{a}_a = 0.23 C_D^{\frac{1}{2}}$ and C_D is based on W. With these approximations the smaller appendage contributions can be estimated and included in the overall wake to lend some structure.

For the turbulent contribution from the appendages, a value of 1.0 is taken for $\sqrt{q_{max}}/u_{d_{max}}$, following Meng and Innis (1977), and this is used in Eq. (9) with the above wake scales.

3.3 Breaking bow wave

The breaking of the bow wave will contribute to an overall deficit wake width which is two to three times the hull beam. The width of the breaking bow wave foam is clearly shown in several photographs in Peltzer (1984a). The analysis of the SIR-B data by Hawkins, Petty and Wheeler (1986) also showed that the SAR wake image near the ship typically was two to three times the ship's beam. Lindenmuth's (1987) data for the DTRC model #5415–1 shows a wake-width for the breaking bow wave that is about 60% to 75% of the model beam on each side of the main hull wake. Thus, the width of the bow wave momentum deficit is taken to be about 75% of the ship beam on each side of the ship hull. Baba (1976) reports the breaking bow wave may account for up to 25% of a ship's total resistance as determined by wake velocity deficit surveys. This is not an additional resistance overall but does appear in the wake deficit rather than in the farfield Kelvin waves. We have provided for an input percentage to be applied to the wavemaking resistance as a means to estimate the total wake deficit due to bow wave breaking. Values can range from a few percent to nearly 100% depending on ballast condition, fullness of the hullform, the Froude number and the local bow geometry. In view of the wide range of variation it is difficult to recommend general values to use in wake simulations. In lieu of any other guidance the fraction due to breaking should be retained as a study parameter. If the user of the model provides no further input for the energy lost to wave-breaking, the percentage applied to the wavemaking resistance is 5%.

The deficit wake due to breaking is treated as an appendage wake using Eq. (1) for the velocity field and Eq. (9) for the turbulence field. The maximum velocity is estimated through the momentum balance in Eq. (2) with the drag specified as above. The horizontal wake scale is taken to be one-half of the beam and the vertical scale determined as in the appendage section. The maximum turbulent kinetic energy is uncertain for a wave breaking process but Duncan (1983) notes an analogy with an ordinary deficit wake where turbulent velocities of a few percent of U_0 are expected. A value of 2% is used for $\sqrt{q_{max}}/U_0$ in the model, but values of q_{max} should be refined based upon data of future experiments.

3.4 Propellers

The propeller contribution to the wake is modeled as a jet with swirl. For jets in which the jet velocity is not much larger than the free stream velocity, the self-similar axial velocity profiles are given by Rajaratnam (1976) as

$$u_p = u_{p_{max}} e^{-\tilde{a}\left(\frac{r}{r_h}\right)^2} \tag{11}$$

where r is the radial distance from the jet centerline, r_h is the jet half width and $u_{p_{max}}$ is the peak value of the thrust velocity, and $\tilde{a}$ is a constant (as before) to fit the curve to the experimental data. For the thrust profile of a self-propelled slender body, Lin and Pao (1974) obtained a best fit of the distribution with $\tilde{a} = 2.3$. Innis (1986) suggests $\tilde{a} = 2.45$ for the case of the over-thrusting propeller jet. For a ship hull, the flow into the propeller disc is influenced by the hull boundary layer, vortices, the wake of the shaft and the supporting struts. Despite these asymmetries in the inflow to the propeller disc, we use this model for the propeller jet with $\tilde{a} = 2.45$ for lack of a better constant. More general data is expected from a series of experiments on propeller jets now underway at the DTRC. Results from the first phase of these experiments (Blanton and Fish - 1988) support the parameters which are being used in our current models.

Lin and Pao (1974) derived the following for the self-similar propeller swirl velocity

$$V_s = V_{s_{max}} \tilde{a}_1 \left(\frac{r}{r_{s_h}}\right) e^{-\tilde{a}_2 \left(\frac{r}{r_{s_h}}\right)^2} \tag{12}$$

where r_{s_h} is the half width for the swirl profile and is frequently different from r_h. They fit their experimental data with $\tilde{a}_1 = 4.56$ and $\tilde{a}_2 = 3.84$. Innis (1986) has found that values of 4.34 and 3.56 have resulted a better fit of some more recent data. The present model uses the values from Innis.

The thrust (T) of the propellers can be obtained by integrating the propeller axial velocity to give

$$T = \frac{\pi}{\tilde{a}} \rho U_0 u_{p_{max}} (r_h)^2 \tag{13}$$

for one propeller. In the model, the thrust of the propellers is determined from the sum of the frictional and wave resistance. As noted above, the model does not have separate provision for contributions to the total resistance from resistance augmentation and form drag.

The angular momentum imparted to the wake by a propeller is obtained by integrating $r\,V_s$ using Eq. (12). This integration leads to an expression for the propeller torque (Q) as

$$Q = \pi \rho U_0 V_{s_{max}} (r_{s_h})^3 \frac{\tilde{a}_1}{(\tilde{a}_2)^2} \tag{14}$$

The thrust and torque can be combined to define the swirl number S (see Rajaratnam – 1976) for swirling jet flows as

$$S = Q/(TD_p/2). \tag{15}$$

where D_p is the propeller diameter. Propeller coefficients for torque and thrust are given by Todd (1967) as

$$K_Q = \frac{Q}{(\rho n^2 D_p^5)}$$

and

$$K_T = \frac{T}{(\rho n^2 D_p^4)}$$

with n being the speed of rotation of the propellers. The swirl number is then related to the propeller coefficients as

$$S/2 = (K_Q/K_T). \tag{16}$$

Hyman (1987) cites values of $0.1 < K_Q/K_T < 0.2$ as representative of the Troost series of propellers. This range of values is supported by data given by Todd (1967) for a range of advance ratios. We take a median value of $K_Q/K_T = 0.15$ for the present model, which yields $S = 0.3$.

In order to finally specify u_{pmax} for use in Eq. (11) and to specify V_{smax} and r_{sh} for use in Eq. (12), we require two more relations in addition to the above thrust and torque conditions. For low swirl number jets the wake scale r_h grows linearly with x. Blevins (1983) gives the following for the wake width of a turbulent axisymmetric jet

$$\frac{r_h}{B} = 0.086\frac{x}{B}. \tag{17a}$$

Specification of the x development of either V_{smax} or r_{sh} permits completion of the modeling of the propeller velocity wake. Most of the data for propeller flows are for self-propelled axisymmetric slender bodies such as the data of Lin and Pao (1974) and Gran (1973). These data suggest that $r_{sh} \propto x^{1/4}$. This growth rate for the swirl half-width is in distinct contrast for that of the axial velocity half-width of a jet. Analysis of the results that Swean (1987b) obtained in the simulations for the DTRC model #5415-1 suggests that r_{sh} should vary as to $x^{1/2}$. Until further data are available, the

following is suggested as the expression for r_{sh}

$$\frac{r_{sh}}{B} = 0.095\left(\frac{x}{B}\right)^{\frac{1}{2}}. \tag{17b}$$

with the constant 0.095 being determined from Swean's (1987b) results.

Lin and Pao (1974) derived the following form for the self-similar turbulence kinetic energy profile in a propeller wake

$$q_p = q_{p_{max}} e^{-\tilde{a}\left(\frac{r}{r_h}\right)^2} \tag{18}$$

and found that $\tilde{a} = 1.38$ fit their data well. Equation (18) is used in the present model with r_h from above and $\sqrt{q_{p_{max}}}/u_{d_{max}} = 0.59$ to account for the turbulence arising from the action of the propeller. Refinements to these models for the propeller wakes are recommended as more data become available.

3.5 Vortices

The final components in a wake are vortices from a number of sources such as the rudder, the hull and the bilge keels. The Lamb vortex (Lamb – 1945, p. 592) combines an irrotational outer region with a rotational core and is given by

$$V_s(r) = \frac{\Gamma}{2\pi r}\left(1 - e^{-\left(\frac{r}{r_c}\right)^2}\right) \tag{19}$$

where Γ is the circulation of the vortex, r is the distance from the vortex center, and r_c is the radius of the rotational core. We adopt this form for the vortex velocity field and assume that the vortices will occur in pairs with opposite circulation. For such a pair of vortices, Sprieter and Sacks (1951) relate the core radius r_c to the vortex separation distance s as $r_c = 0.0775\,s$ and Sarpkaya (1983) reports similar values .

In steady forward motion, the only vortices should be the so-called bilge vortices. There are some differences of opinion as to the source of the bilge vortices. Landweber and Patel (1979) suggest that the occurrence of bilge vortices is a function of the bow geometry and that the bilge vortices may be formed when "the crossflow is large at the turn of the bilge." Others, for example Swanson (1984), attribute the bilge vortices to the "set-down" or "squat" of the hull. Swanson develops the following expression for

the circulation of the bilge vortices

$$\Gamma = \frac{C_p U_0 L}{2f} \tag{20}$$

where L is the hull length, f is the separation of the bilge vortices as a fraction of the beam, and C_p is the hull pressure coefficient for "super velocity" flow as given by Hoerner (1965)

$$C_p = 1.5\left(\frac{B}{L}\right)^{3/2} \tag{21}$$

For a hull form typical of a destroyer, a useful approximation for f is $\pi/4$ which corresponds to an elliptical loading as given by Sprieter and Sacks (1951).

Calculations using Eq. (20) for the bilge vortex circulation give extremely large vortex velocities. Swanson gives an example for a ship 100 m in length, 10 m beam, 5 m draft, and U_0 of 10 m/sec. For this example, he calculates the the circulation is 47 m^2/sec and the swirl velocity at the surface as 2.1 m/sec; consequently at 1 m from the vortex center, the velocity would be more than 7.5 m/sec. While experimental data for ships wakes, even at model scale, are extremely rare, those tests do not support the existence of vortex velocities of this magnitude. It seems necessary to reduce the swirl velocities for the bilge vortices, and one of the input variables for the programmed model adjusts the peak value of the bilge vortex circulation and thus the peak swirl velocity. The default value for the bilge vortex circulation strength is 5% of the value obtained from Eq. (20).

For rudders, bilge keels and other appendages, we use potential flow theory and relate the circulation to the lift coefficient C_L by

$$\Gamma = 4bU_0 C_L/\pi a_r \tag{22}$$

where b is the lifting surface half span, C_L is given by $2\pi \sin\alpha$, α is the angle of attack, and a_r is the effective aspect ratio of the lifting surface.

Appendage vortices are located at the appendage end points but closer together by the factor of $\pi/4$ that is typical of fully formed vortices (see Sprieter and Sacks - 1951). For the bilge vortices, it is suggested that the vortex centers be placed at about the corner of the hull, allowing for some rise and some movement closer together. For

the DTRC model #5415-1 (a high speed destroyer model), for example, the placement would be at $y/D = 0.1$ and $z/B = \pm 0.4$.

3.6 Propeller shaft inclination

If the propeller shafts are inclined from the horizontal, and since combatants usually have differing angles for each shaft, the propeller jets should also be skewed. Hyman (1987) treats the propeller wakes as jets injected downward at a slight angle which produces a downward shift in the jet centerline by the initial data plane. Meng (1985) rotates the inclined propeller jet thrust and swirl components into the ship coordinates. Any adjustments of this nature should include the inclination differences between shafts which may be a significant fraction of the average. However, such an approach neglects the upwelling flow under the aft portion of the hull. Saunders (1957) cites experimental data which show the propeller jets being swept upward by the uprising flow at the stern of the ship model. In that example, it would appear that the angle(s) of the propeller shafts with respect to the horizontal was a less significant effect than the flow angle under the rear portion of the hull. Jets injected at angles to the free stream are also distorted in cross-sectional shape.

The interaction of the hull flow with the propeller jet could be very significant in the development of the ship's far wake. This is particularly true for even weak asymmetric features which will have a large distance over which to distort a highly structured wake. It is probable that future experimental data such as that which will come out of the DTRC experimental program on propeller wakes will increase our understanding of this area of interaction. For the present, the model aligns the propelier wake with the horizontal. This approach should be modified when a more complete understanding of the development of the propeller wake is available.

4. WAKE MODEL

The preceding section describes the basic elements and constraints which will be used in the model for generating a set of initial condition data to be used in a simulation of a ship's far wake. This section describes how the basic elements are assembled and implemented in a computer code. The code is called SURFIN for surface wake initialization.

The resultant mean velocity profiles are a sum of the individual component values at the desired grid locations. Uniform grid spacing is imposed but the increment and ranges can vary in each direction as specified in the input list. The local value of turbulent kinetic energy is taken as the sum of individual components. Hyman

computed component values from the velocity gradients under the assumption of a constant turbulent eddy viscosity. The total turbulence kinetic energy at a particular location was then taken as the maximum value of any component at that location. Owing to the separations between maxima of the various components, he observed that this was not significantly different from a simple summation. We have opted for the simple summation and found that this procedure seems to be satisfactory for the only available data, that of the DTRC model #5415–1.

Application of the several models discussed in the preceeding sections results in superposed velocity (u, v, w) and turbulence kinetic energy (q) fields. Most parabolic marching codes are based on two-equation turbulence models and require an additional transport variable related to the dissipation length scale. If the turbulence model is the standard k, ϵ model, then the additional transported quantity is the isotropic dissipation function ϵ which is related to the turbulent energy via $\epsilon \sim q^{3/2}/l_d$. The turbulent shear strsses are then calculable (to lowest order) from the constitutive relations (Baker – 1982):

$$\overline{u'v'} = -\nu_t \frac{\partial u}{\partial y} \tag{23a}$$

$$\overline{u'w'} = -\nu_t \frac{\partial u}{\partial z} \tag{23b}$$

$$\overline{v'w'} = -\nu_t \left(\frac{\partial v}{\partial y} + \frac{\partial w}{\partial z} \right) \tag{23c}$$

where the turbulent kinematic viscosity is given by $\nu_t = cq^2/\epsilon$ with the constant $c \sim O(0.1)$. Baker (1982), for example, gives $c = 0.068$.

Hyman estimates an eddy viscosity, ν_t, for the flow field, calculates q from the eddy viscosity estimate and the gradient of the mean axial velocity, and then calculates ϵ from the relation $\epsilon = 0.09\, q^2/\nu_t$. Swean (1987a–b), on the other hand, attempts to estimate l_d from the measured shear stress data and then compute ϵ and ν_t. These approaches are similar but we adopt the latter since we feel it is easier to relate l_d to geometric properties of the vessel. Swean (1987a) examined the measured shear stress distributions for drag and self-propelled slender bodies and compared them to values obtained from Eqs. (23) using l_d as a parameter. For the drag wakes he obtained good agreement with $l_d = 0.2D$ where D is the characteristic diameter of the wake producing body. The agreement was not so good, however for the self-propelled configurations, especially near the edges of the swirl region where the measured shear exhibited a significant tangential component not supported by the mean velocity gradient data. A similar analysis applied to the data of Lin and Pao (1974) and Gran (1973) results

in $l_d = 0.63D$ for the former and $l_d = 0.85D$ for the latter as values yielding good correlations between measured stress and turbulent kinematic viscosity. In terms of the propeller diameter, D_p, these scale lengths are $1.46D_p$ for Lin and Pao's results and $1.79D_p$ for Gran's data.

In a similar analysis for a surface ship model, Swean (1987b) found that a scale of 23% of the beam width (or 85% of the propeller diameter) provided a good correlation between the turbulence kinetic energy and the measured stresses. Based on the above considerations, the model employed in the current wake initiator will compute the length scale and thus the dissipation function as a fraction (25%) of the geometric scale L_ϵ input by the user. In the absence of an input for L_ϵ, the scale will default to $0.25B$. Using the prescribed scale and the superposed fields for q, u, v,and w, the shear stress field

$$\tau_x = \frac{1}{U_0^2}\sqrt{\left(\overline{u'v'}\right)^2 + \left(\overline{u'w'}\right)^2}$$

is developed from Eqs. (23). A provision is included in the program to allow the user to meet alternative constraints on the shear stress by interactively manipulating the characteristic (maximum) value of the above composite stress field through varying L_ϵ.

Finally, it should be noted that the initial mean flow velocities u, v and w have been independently specified and are not divergence free. The parabolic codes in use at NRL have options to operate on the input data to condition the velocities prior to initiating the marching procedure, and it is assumed that such is the case for most such codes. It would be a simple matter to incorporate such a mechanism into SURFIN but the resulting code would be several times the size of the present one and consequently this has not been done. In a following section we show by example the typical adjustments made to the velocity field by such procedures.

5. PROGRAM INPUT

Program SURFIN is designed to accept data input either from a data file, or from the user's terminal. In either case, data are read on logical unit 5, terminal or line printer data are written to logical unit 6, and the profile data are written to logical unit 22. Most operating systems such as UNIX and VMS allow a user to direct unit 5 input either from a terminal or a file and allow unit 6 output to go to either a terminal or a file. The user will probably find it more convenient to prepare a data file and make changes as desired in the file. Table I is an example of a data file for the DTRC model #5415–1 (a high speed destroyer model). The program input is list directed

(free format) with one or two values per line. Each line in the table includes a brief descriptor of the data item. This table can be used as a template for developing other data files. The units for the data items are as indicated in the file.

SURFIN first asks if the input is to come from the file or the terminal. Responses other than `term` or `file` are considered invalid and the question is repeated, although a response of `stop` is allowed to end program execution. For file input, the program eliminates further prompts and simply reads the file in sequence. The following input description is worded as if the response to the initial question is `term`.

SURFIN next asks for the name of the output file and opens that file. The user is then asked which of the wake elements the program is to use in assembling the initial condition data so that the user can examine individual parts of the wake. The wake elements are, in order, the hull, the propeller thrust, the propeller swirl velocity, the appendage wakes, the appendage vortices, and the bilge vortices. The user selects the wake elements to be considered by entering an integer `1` for each wake element to be included and an integer `0` for each element to be excluded. Next, the user is asked for an adjustment factor for the bilge vortex circulation strength. The program is coded to use only 1/20 of the Eq. (20) amount and a response of `1.0` leaves that unchanged: a response of `2.0`, for example, doubles that amount. The input data for the hull, propellers and appendages are then read. If the input is coming from a terminal instead of from a file, the program will prompt for changes to L_ϵ after the u, v, w, and q profiles are calculated.

6. PROGRAM OUTPUT

After calculating the velocity components and the turbulence kinetic energy of the wake elements, the programs calculates the dissipation function ϵ from the input value of L_ϵ. The composite stress field is then calculated and the maximum value of τ_x is written to logical unit 6. If the input data are coming from a terminal, the program asks if the user wishes to change L_ϵ. At a `yes` response, the program prompts for a new value, recalculates the dissipation function and stress field, and again displays the maximum of τ_x and asks if the user wishes to change L_ϵ. After a `no` response, the program calls subroutine `UNFORM` to write to the output file the values of the coordinates, the velocity components, the turbulence kinetic energy and the dissipation function. The routine `UNFORM` is called once for each velocity component and each turbulence quantity. The output data are written in a manner which matches the input requirements of the PLOT3D and PLOTC programs at NRL. The output data are written to the output file in the order of coordinates and then dependent variable for each call to the subroutine. The user can easily change the output format to match particular requirements. The

output data are nondimensionalized by the appropriate powers of the ship speed (U_0) and the length scale (B).

7. RESULTS AND DISCUSSION

There is little data with which the results of program SURFIN can be compared. Lindenmuth (1987) at the DTRC has made detailed measurements of the wake of a twin-screw high speed destroyer model (model #5415–1). These data have not yet been published but portions are available. The locations and dimensions of the principal wake generating elements are given in Table I and the stern view of the model #5415–1 is shown in Fig. 1. The initial condition data from SURFIN are presented here for the model data plane at $x = 10\ ft$, or in program coordinates, approximately $4B$.

Wakes of the individual components are shown and then composite wakes formed by superposition of the individual wakes are shown. The profile data are shown in the same format used by Swean (1987b) in that only the results for the starboard half plane are shown. As in Swean, the vertical range is $-0.8\,B$ to 0.0 and the horizontal coordinate range is 0.0 to $1.2\,B$. Figure 2 shows contour plots of the axial velocity deficit and turbulence kinetic energy for the bare hull without appendages or propellers. The wakes for the rudders are shown in Fig. 3 and for the bilge keels and breaking bow waves in Fig. 4. The wake of the propellers with the propellers turning inboard are shown in the next two figures. Figure 5 shows the axial velocity and turbulence and Fig. 6 shows the transverse velocities by a vector plot of V_s, where V_s is given by

$$V_s \equiv \frac{1}{U_0}\left(v^2 + w^2\right)^{1/2}.$$

The propeller wakes are for the thrust equal to the combined values of frictional and wave resistance. Figure 7 shows the swirl velocities for the bilge vortices with only 1/20 of the amount of circulation from Eq. (20) being used. At this level of reduction, the peak swirl velocity for the bilge vortices is 40% of the peak of the propeller swirl velocity.

The composite wake of the hull, rudders, bilge keels and breaking bow wave is shown in Fig. 8. As the appendages are aligned with the main flow, there are no tranverse velocities generated for this configuration. Although bilge keels were not included on the tested model (Lindenmuth - 1988), they have been included to this point to demonstrate what the effect of bilge keels might be on the initial profile data and to demonstrate the capability of the SURFIN code to give the wake of appendages

angled to the horizontal or vertical. Without the bilge keels, the wake of the hull with rudders and breaking bow wave is shown in Fig. 9.

The wake axial velocity and turbulence energy for the self-propelled hull are shown in Fig. 10. Without the inclusion of the bilge vortices, the transverse velocities are as in Fig. 6.

Inclusion of bilge vortices will change only the transverse velocity flow fields. A composite of the swirl velocities for the propellers and bilge vortices is shown in Fig. 11. The rotational directions of the propeller swirl and the bilge vortices are opposite, and the peak swirl velocity is greater than for either component since the flows reinforce between the neighboring centers.

For comparison, we include three figures based on Lindenmuth's experimental data. Figure 12 (which is Fig. 9a of Swean - 1987b) shows the axial velocity distribution, Fig. 13 (Swean's Fig. 10a) shows the turbulence kinetic energy, and Fig. 14 (Swean's Fig. 11a) shows the swirl velocities. Comparing the axial velocities in Figs. 10a and 12 shows that the minimum velocity in the hull wake and the peak velocity in the propeller wake have lower values in the results from SURFIN than in the experimentally based data. The minimum velocities are $(u - U_0)/U_0 = -0.094$ in the SURFIN results and -0.125 in the experimental data. The maximum velocities are $(u - U_0)/U_0 = 0.077$ in the SURFIN results and 0.11 in the experimental data. The experimental data show a broader deficit wake than the SURFIN results. Also seen in the experimental data is an upwelling of overthrusted fluid in the center of the hull wake. The basis of the model used in SURFIN is linear superposition of the individual wake components, and nonlinear interactions in the near wake region are not modeled. Allowing for this basic limitation of the model, the results from SURFIN seem to compare well with the experimental data.

The turbulence kinetic energy as seen in Figs. 10b and 13 compare more favorably. The peak values are quite close, $q/U_0^2 \times 10^4 = 54$ and 58 for the SURFIN and experimental data respectively. The values of q at the surface are also quite similar. The experimental data show greater turbulence in the wake of the breaking bow wave than do the SURFIN results. In view of the differences in the axial velocities, this level of agreement for the turbulence kinetic energy is not expected. The amount of turbulence from the SURFIN model is directly influenced by the values chosen for $\sqrt{q_{max}}$. The value of $0.59\,u_{d_{max}}$ for the propeller is from Lin and Pao (1974) and better data are not available. For the hull, the value of $0.3\,u_{d_{max}}$ is taken as an intermediate value. Increasing this value raises the level of turbulence in the SURFIN results and decreasing it lowers the level of turbulence. From Figs. 5b and 9b, it is seen that the propeller wake

contributes most of the turbulence in the current model and changes in the amount of turbulence contributed by the hull has only a small effect.

In the swirl velocities in Figs. 6 and 14, the results from SURFIN show a slightly larger region for the propeller swirl and a slightly higher value for $V_{s_{max}}/U_0$ than do the experimental data. The SURFIN results give a value of 0.066 and the experimental data give 0.063. We note that the close agreement for the swirl velocities is based on the use of Eq. 17b which was determined from Swean's (1987b) simulations for the DTRC model #5415–1. For the propellers turning outboard, the SURFIN model gives the same swirl velocities as for the propellers turning inboard, whereas the experimental data of Lindenmuth (1987) give swirl velocities 50% higher for the propellers turning outboard.

In Fig. 14, bilge vortices are not evident, although the data for the unpropelled model and for the self-propelled model with the propellers turning outboard seemed to show distinct bilge vortices, even though the model did not have bilge keels. Figure 14 does show a distinct counter rotating vortex above and to the inboard of the propeller vortex. This latter vortex may be induced by the propeller vortex and be the source of the upwelling of the overthrusted fluid seen in Fig. 12. The counter rotating vortex above the propeller vortex and the upwelling of overthrusted fluid are examples of the very non-linear interactions that can occur between wake components in the near wake region. The SURFIN model does not account for such complex and non-linear effects. Since the SURFIN model yields an idealized representation of the beginning of the far wake, predictions of the far wake using PNS codes initialized with the SURFIN model results are idealized representations of the far wake. Future improvements to the SURFIN model, which will give more realistic results, will yield more realistic predictions of the far wake.

As we pointed out in a previous section, the velocity field is not divergence free. The documentation of the parabolic marching code SURFWAKE (Meng and Innis – 1977 and Meng, Grant and Ulman – 1985), for example, describes a procedure for adjusting the velocity field on the finite grid so that the resulting field approximately satisfies the continuity equation. The procedure does this primarily by adjusting the v and w components while other field variables undergo only very small adjustments. Figure 15 is the adjusted swirl velocity field after being processed by the pre-processor in SURFWAKE. It is seen that in this case, the characteristic magnitude of the swirl velocity is adjusted upward by about 9% (compare with Fig. 6). Such a procedure could be made an integral part of SURFIN but to this point has not been done since the PNS codes generally have their own mechanisms to insure internal consistency of the input fields.

8. SUMMARY AND CONCLUSIONS

An approximate model has been developed for generating a set of initial condition data for the numerical simulation of a surface ship's far wake. The model has been implemented in the code SURFIN and includes elements for modeling the major components of a ship's wake. Comparison of the generated initial condition data with experimental data for the model #5415-1 shows that the present model gives reasonable initial data for simulating such a ship's far wake. For cases where experimental or model scale data are not available, this model should be most useful in providing initial data for simulation of the far wakes.

Two areas of concern have been dealt with only lightly thus far – the bilge vortices and the propeller wake alignment. As noted above, the bilge vortex model of Swanson gives very large swirl velocities. While some experimental data do seem to show bilge vortices, the swirl velocities are much lower than would be given by Swanson's model. Two areas have been identified that could be a source of the Swanson model overestimating the swirl velocity. The relations from aerodynamics relating circulation and lift and vortex separation are for high aspect ratio wings. A ship hull is certainly not a high aspect ratio wing. At best, it might be considered as a very low aspect ratio wing. Applying the modifications for low aspect ratio wings to Swanson's model for circulation still gives very large swirl velocities. More likely, the C_p which corresponds to the hull "super velocity" should not be equated to a lift coefficient and used to calculated circulation. It is probably more reasonable to consider that particular C_p as the source generating much of the nearfield wave system. Also of concern is whether a displacement hull might be considered as a wing at all.

Of equal uncertainity is the appropriate alignment of the propeller wake. There should be an effect from the inclination of the propeller shafts and probably equally (or more so) there should be an effect from inclinations of the flow streamlines around the stern of the vessel. There is very little data to indicate how much effect either factor should have. Experimental data are needed which will contribute to a better understanding of both of these areas of uncertainty. When such data become available, the present model can be refined.

9. ACKNOWLEDGEMENTS

The authors acknowledge the support of the Office of Naval Research (Code 12), the Naval Research Laboratory, the David Taylor Research Center, and the University of Michigan for the support for this project through the Ship Wake Consortium. The authors also acknowledge the helpful suggestions and comments of Dr. William C. Sandberg.

10. REFERENCES

Baba, E., 1969, "A New Component of Viscous Resistance of Ships", Journal of the Society of Naval Architects of Japan, Vol.125, pp. 23-34.

Baba, E., 1976, "Wave Breaking Resistance of Ships", International Symposium on Wave Resistance, Tokyo.

Baker, A. J., 1982, "The CMC/3DPNS Computer Program for Prediction of the Three-Dimensional, Subsonic, Turbulent Aerodynamic Juncture Region Flow; Volume 1 - Theoretical", CR 3645, National Aeronautics and Space Administration, Hampton, Virgina.

Blanton, J. N. and S. Fish, 1988, "Near and Far Field Propeller Wake Study Using Laser Doppler Velocimetry," report DTRC SHD 1268-01, David Taylor Research Center, Washington, D. C.)

Blevins, R. D., 1983, *Applied Fluid Dynamics Handbook*, Van Nostrand Reinhold, New York.

Chevray, R., 1968, "The Turbulent Wake of a Body of Revolution," Transactions of the ASME, Journal of Basic Engineering, June 1968, pp. 275-284.

Chevray, R. and Kovasznay, L. S. G., 1969, "Turbulence Measurements in the Wake of a Thin Flat Plate," AIAA Journal, Vol. 7, pp. 1641-1643.

Duncan, J. H., 1983, "The Breaking and Non-breaking Wave Resistance of a Two-dimensional Hydrofoil," Journal of Fluid Mechanics, Vol. 126, pp. 507-520.

Gran, R. L., 1973, "An Experiment on the Wake of a Slender Propeller-Driven Body," TRW Report 20086-6006-RU-00, Trw Systems Group, Redondo Beach, California.

Innis, G. E., 1987 private communication, Scientific Applications Inc., La Jolla, California.

Kuo, Y-H. and Baldwin, L. V., 1966, "Diffusion and Decay of Turbulent Elliptic Wakes", AIAA Journal, Vol. 4, pp. 1566-1572.

Hawkins, S., A. F. Petty and C. S. Wheeler, 1986, "Sea-Surface Signiture Experiment SIR-B/K1049 (U)," NRL Report 9003, Naval Research Laboratory, Washington, D. C., (Confidential).

Hoekstra, M., 1974, "Prediction of Full Scale Wake Characteristics Based on Model Wake Survey", Symposium on High Powered Propulsion of Ships, Wageningen, The Netherlands.

Hoerner, S. F., 1965, *Fluid Dynamic Drag*, published by the author, Brick Town, New Jersey.

Hyman, M., 1987, "Initial Data Plane Estimation for Surface Ships - II," NCSC TN (to be published), Naval Coastal System Center, Panama City, Florida.

Lamb, H., 1945, *Hydrodynamics*, 6th ed.(1932), Dover, New York.

Landweber, L. and V. C. Patel, 1979, "Ship Boundary Layers," Annual Review of Fluid Mechanics, Vol. 11, pp. 173-205.

Lin, J. T. and Y. H. Pao, 1974, "The Turbulent Wake of a Propeller- Driven Slender Body in a Non-Stratified Fluid," Flow Research Report No. 14, Flow Research Inc., Kent, Washington.

Lin, J. T. and Y. H. Pao, 1979, "Wakes in Stratified Fluids," Annual Review of Fluid Mechanics, Vol. 11, pp. 317-338.

Lindenmuth, W. T., 1987, private communication, (data on model #5415–1 model tests to be published as report DTRC SHD 1273-01 "Viscous Macro-Wake Behind a Twin-Screw High Speed Surface Ship," Sept. 1988, with D. J. Fry).

Lindenmuth, W. T., 1988, private communication.

Meng, J. C. S. and G. E. Innis, 1977,"User's Manual for the Computer Program FAST-WAKE: A Fast and Accurate Code for Simulation of the Stratified Turbulent Wake Flows," SAI-77-864-LJ, Sciance Applications, Inc.,La Jolla, California.

Meng, J. C. S., J. R. Grant and J. S. Ulman, Jr., 1985, "Numerical Simulation of Turbulent Wake with a Free Surface Phase I: SURFWAKE Implementation and Implementation of a Towed Wake," Gould report OSD-771-HYDRO-CR-85-05, Gould Defense Systems Inc., Middletown, Rhode Island.

Milgram, Jerome H., "Theory of Radar Backscatter from Short Waves Generated by Ships with Application to Radar (SAR) Imagery" Journal of Ship Research, Vol. 32, No. 1, pp. 54-69.

Mitra, P. S., W. L. Neu and J. A. Schetz, 1985, "Effect of a Free Surface on the Wake of a Slender Body," report VPI-AERO-146, Virginia Polytechnic Institute and State University, Blacksburg, Virginia.

Pao, Y. H. and J. T. Lin, 1973a, " Turbulent Wake of a Towed Slender Body in Stratified and Nonstratified Fluids: Analysis and Flow Visualization ." Flow Research Report No. 10, Flow Research Inc., Kent, Washington.

Pao, Y. H. and J. T. Lin, 1973b, "Velocity and Density Measurments in the Turbulent Wake of a Towed Slender Body in Stratified and Nonstratified Fluids," Flow Research Report No. 12, Flow Research Inc., Kent, Washington.

Peltzer, R. D., 1984a, "White-Water Characteristics of Surface Vessels," Memorandum Report 5335, Naval Research Laboratory, Washington, D. C.

Peltzer, R. D., 1984b, "Remote Sensing of the USNS HAYES Wake," Memorandum Report 5430, Naval Research Laboratory, Washington, D. C.

Rajaratnam, N., (1976), *Turbulent Jets*, Elsevier Scientific Publishing Co., New York.

Ramberg, S. E., T. F. Swean, Jr. and M. W. Plesniak, 1988, "Turbulence in a 2D plane jet at a free surface", Memorandum Report in preparation, Naval Research Laboratory, Washington, D. C.

Sarpkaya, T., 1983, "Trailing vortices in homogeneous and density-stratified media", Journal of Fluid Mechanics, Vol. 136, pp. 85-109.

Saunders, H. E., 1957, *Hydrodynamics in Ship Design*, VOLUME 2, Society of Naval Architects and Marine Engineers, New York.

Schlichting, H., 1968, *Boundary Layer Theory*, Sixth Edition, McGraw Hill, New York.

Scully-Power, P., 1986, "Navy Oceanographer Shuttle Observations: STS 41-G Mission Report", Technical Report No. 978, Naval Underwater Systems Center, New London.

Sprieter, J. R., and A. H. Sacks, 1951, "The Rolling Up of the Trailing Vortex Sheet and Its Effect on the Downwash Behind Wings," Journal of the Aeronautical Sciences, Vol. 18, No. 1, pp. 21-32.

Swain, L. M., 1929, "On the Turbulent Wake behind a Body of Revolution," Proceedings of the Royal Society, London, Series A, Vol. 125, pp. 647-659.

Swanson, C. V., 1984, "Radar Observability of Ship Wakes," Memorandun Report, Swanson & Associates.

Swanson, R. C., Jr., J. A. Schetz and A. K. Jakubowski, 1974, "Turbulent Wake behind Slender Bodies including Self-Propelled Configurations," report VPI-AERO-024, Virginia Polytechnic Institute and State University, Blacksburg, Virginia.

Swean, T. F., Jr., and R. D. Peltzer, 1984, "Free Surface Effects on the Wake of a Flat Plate," NRL Memorandum Report 5426, Naval Research Laboratory, Washington, D. C.

Swean, T. F.,Jr., 1987a, "Calculations of the Turbulent Wake behind a Slender Self-Propelled Double-Body and Comparisons with Experiment," NRL Memorandum Report 6075, Naval Research Laboratory, Washington, D. C.

Swean, T. F.,Jr., 1987b, "Numerical Simulations of the Wake Downstream of a Twin-Screw Destroyer Model ", NRL Memorandum Report 6131, Naval Research Laboratory, Washington, D. C.

Tagori, T., 1966, "Investigations on Vortices Generated at the Bilge", Proceedings of the Eleventh ITTC, Tokyo.

Todd, F. H., 1967, "Chapter 7, Resistance and Propulsion," of *Principals of Naval Architecture*, J. P. Comstock, Editor, Society of Naval Architects and Marine Engineers, New York.

Watson, K. M., 1987, "Note Concerning: Turbulent and Vortex Wakes of Surface Ships", Mitre Corporation, JSN-87-8501.

TABLE I

```
file                input from file
outdat              main output file
outdatm             Temp file  for vector plots
1 1 1 1 0 0    include hull, prop thrust, prop swirl & appndg drag
 1.0           adjust bilge vortex strength (1.0 => 1/20 of Swanson)
 2.492         beam       feet       c  beginning of nddw data
 0.6667        width of transom as fraction of beam
 0.817         draft      feet
 18.80         length     feet
  1185.0       displacement  lbf (weight)   (calculate if zero)
  53.705       wetted area   ft^2           (calculate if zero)
 6.756         speed      feet per second
  0.0          kelvin drag  lbf             (calculate if zero)
  0.0          viscous draq  lbf            (calculate if zero)
 4.0           location of initial data plane in beams (-10 ft)
 2             # props       (inboard rotation)
  140.0         rpm  (for estimate of horsepower required)
 -1            rotation  (counter-clockwise facing forward)
 +0.171        yc   fraction of draft above keel
  0.222        zc   fraction of beam from CL                starboard
  0.28         propeller diam / beam
 +1            rotation  (clockwise facing forward)
 +0.171        yc   fraction of draft above keel
 -0.222        zc   fraction of beam from CL                port
  0.28         propeller diam / beam
  0.5          r_hs spreading power
  1            include breaking wave generators as last 2 app  (1=y, 0=n)
 4              # appendages  (2 less if breaking bow waves are included)
  0.081 .88    yl & y2       fraction of draft above keel     rudders
  0.167 .167   zl & z2       fraction of beam from CL
  0.0           angle of attack (for vortices)
  5             thickness    percent of beam
  2.0           prcdrag      percent of viscous drag
  0.081 .88    yl & y2       fraction of draft above keel     rudders
 -0.167 -.167  zl & z2       fraction of beam from CL
  0.0           angle of attack (for vortices)
  5             thickness    percent of beam
  2.0           prcdrag      percent of viscous drag
  0.21  .66    yl & y2       fraction of draft above keel     bilge keels
  0.417 .278   zl & z2       fraction of beam from CL
  0.0           angle of attack (for vortices)
  2             thickness    percent of beam
  0.5           prcdrag      percent of viscous drag
  0.21  .66    yl & y2       fraction of draft above keel     bilge keels
 -0.417 -.278  zl & z2       fraction of beam from CL
  0.0           angle of attack (for vortices)
  2             thickness    percent of beam
  0.5           prcdrag      percent of viscous drag
  0.95  .95    yl & y2       fraction of draft above keel     breaking wave
  0.500 1.25   zl & z2       fraction of beam from CL
  0.0           angle of attack (for vortices)
  3             thickness    percent of beam
  5.0           prcdrag      percent of wave drag
  0.95  .95    yl & y2       fraction of draft above keel     breaking wave
 -0.50 -1.25   zl & z2       fraction of beam from CL
  0.0           angle of attack (for vortices)
  3             thickness    percent of beam
  5.0           prcdrag      percent of wave drag
  0.1           y       for bilge vortices, fraction of draft above keel
 -0.4  0.4      zl & z2 for bilge vortices, fraction of beam from CL
  0.25          L_eps  in beams  length scale for dissipation
```

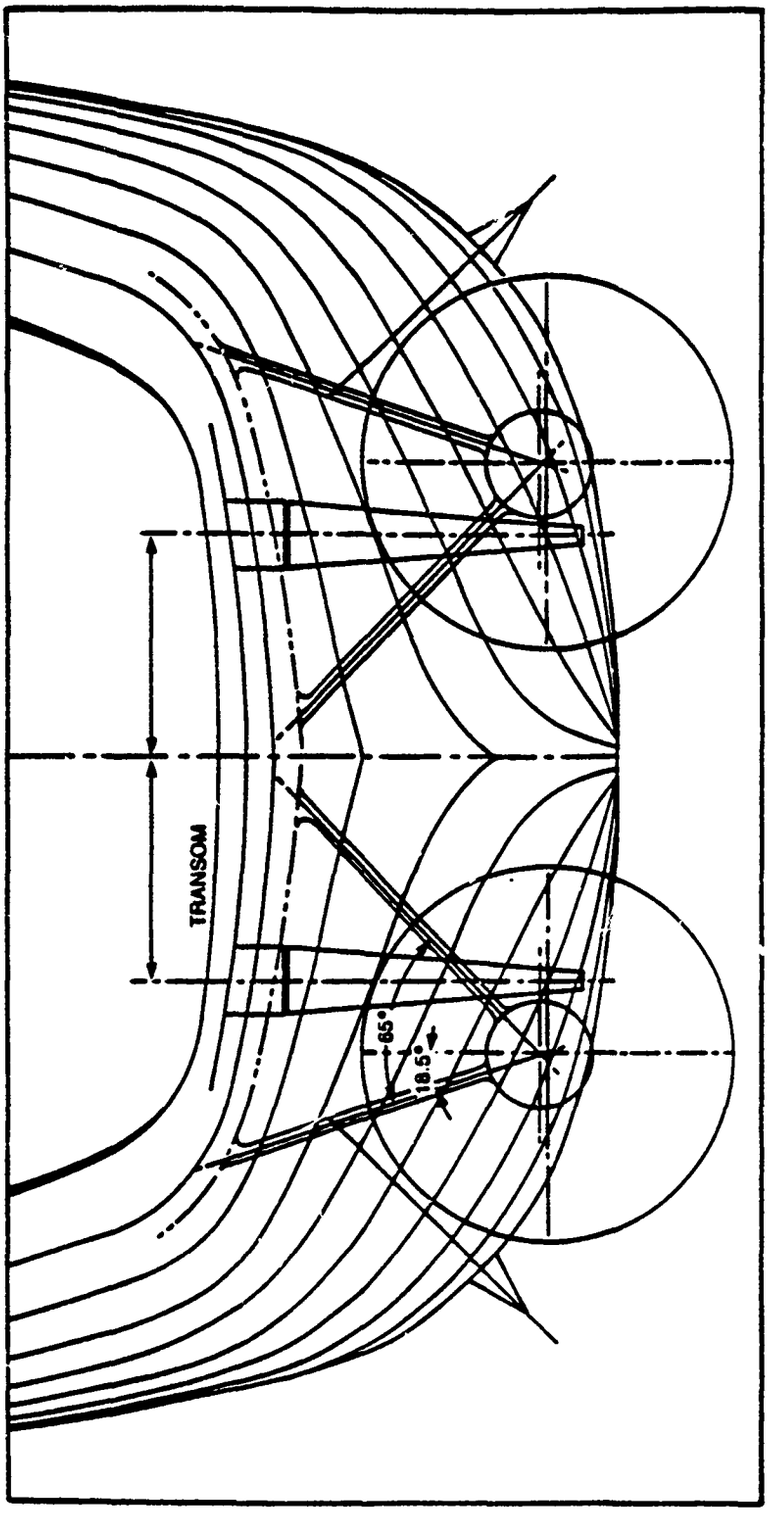

Fig. 1 — Stern view of wake generating elements of high speed ship model

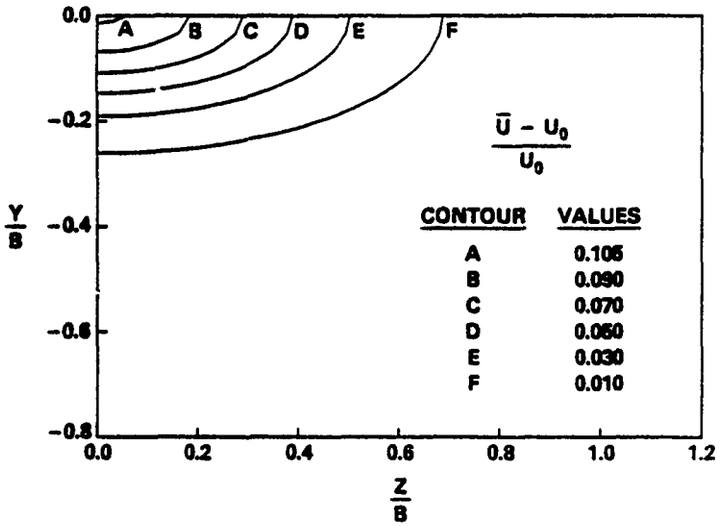

(a) Contours of normalized mean axial velocity deficit

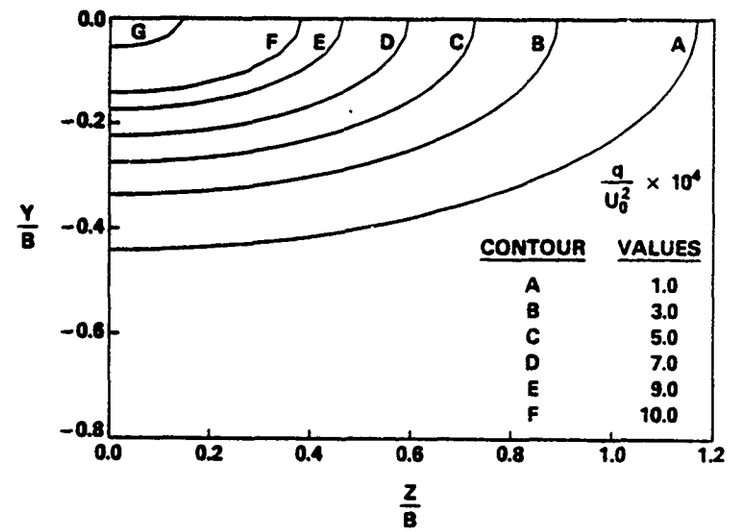

(b) Contours of turbulence kinetic energy

Fig. 2 — Distributions of Initial Profile Data — wake of hull only

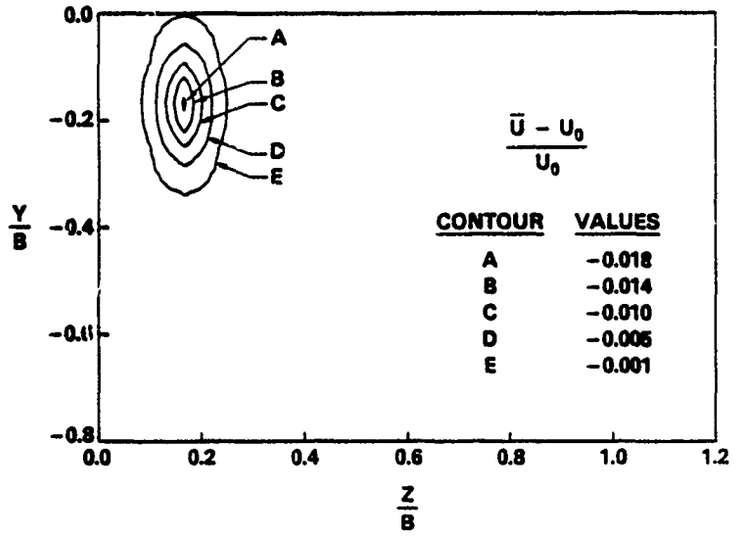

(a) Contours of mean streamwise velocity

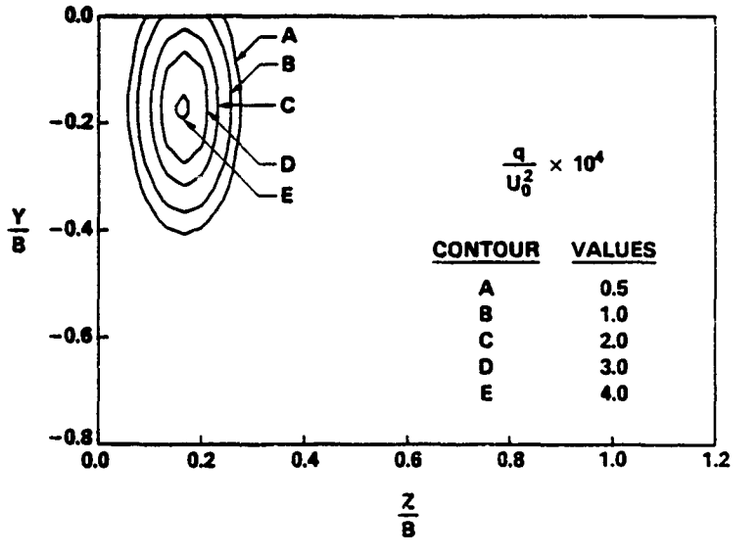

(b) Contours of turbulence kinetic energy

Fig. 3 — Distributions of Initial Profile Data — wake of rudder only

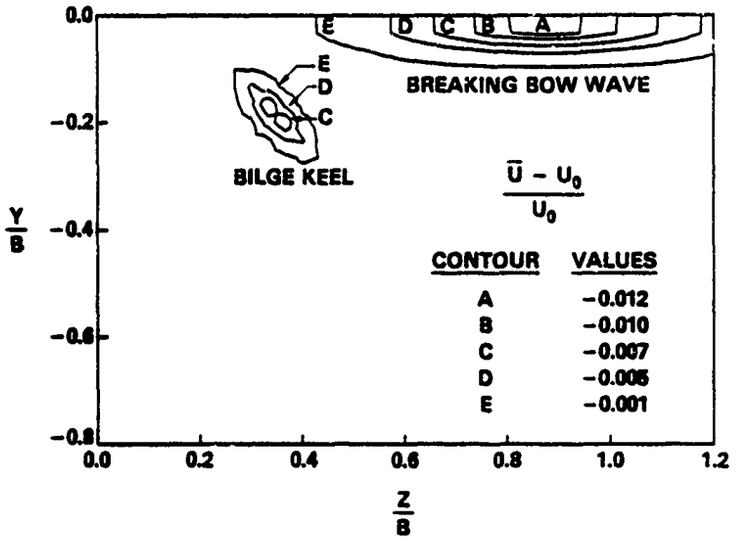

(a) Contours of mean streamwise velocity

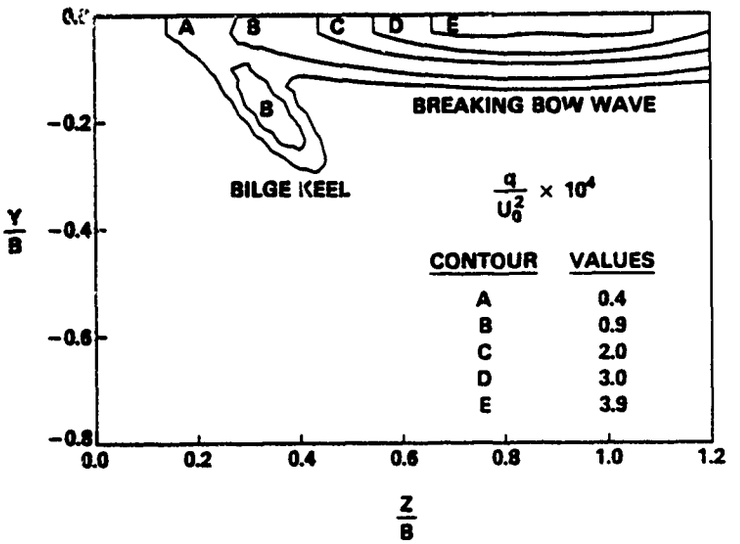

(b) Contours of turbulence kinetic energy

Fig. 4 — Distribution of Initial Profile Data — wake of bilge keel and breaking bow wave

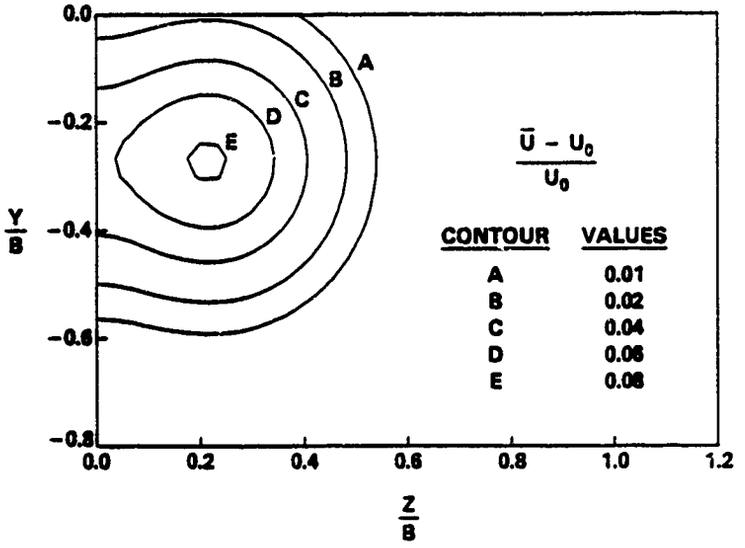

(a) Contours of mean streamwise velocity

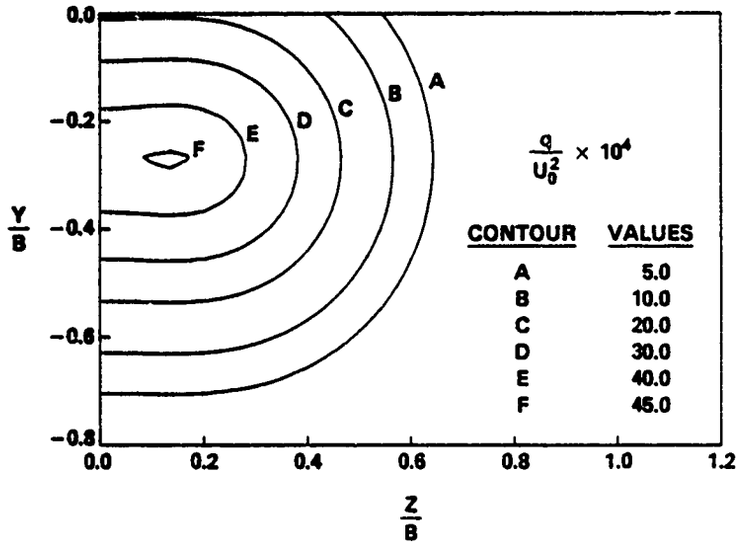

(b) Contours of turbulence kinetic energy

Fig. 5 — Distributions of Initial Profile Data — wake of propeller only

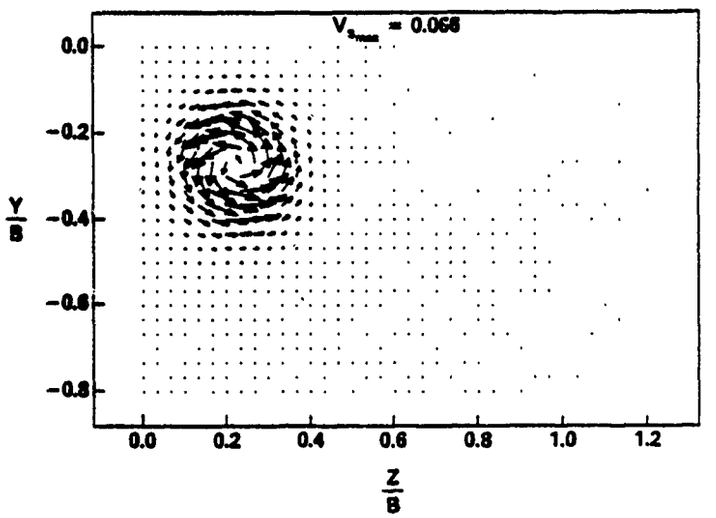

Fig. 6 — Distribution of Initial Profile Data — propeller swirl velocity vectors

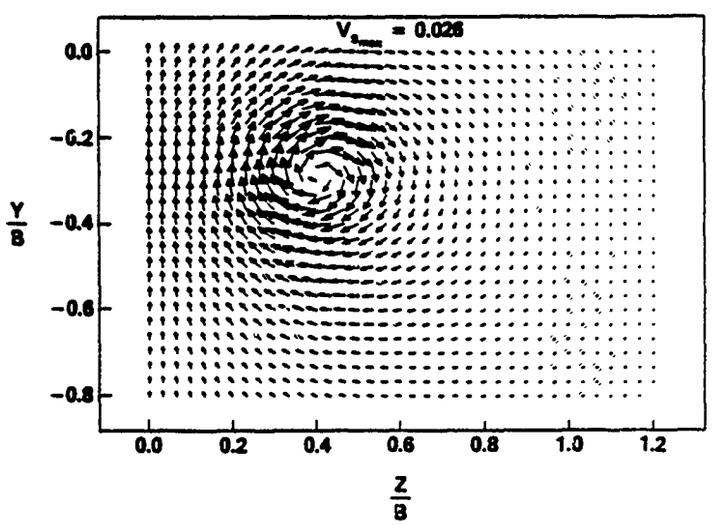

Fig. 7 — Distribution of Initial Profile Data — bigle vortex velocity vectors

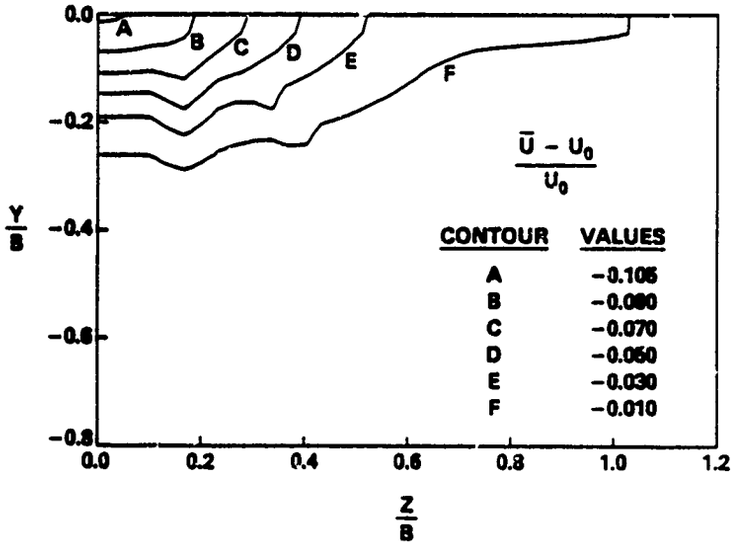

(a) Contours of mean streamwise velocity

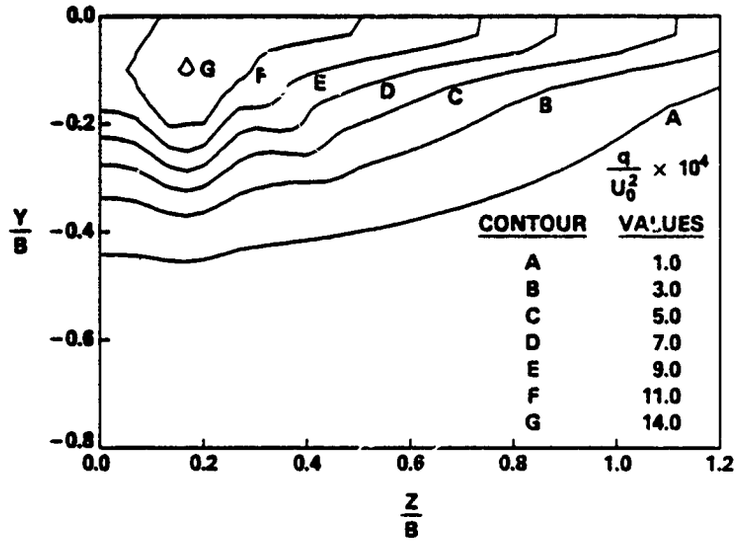

(b) Contours of turbulence kinetic energy

Fig. 8 — Distributions of Initial Profile Data — wake of hull, bilge keel, rudder and breaking bow wave

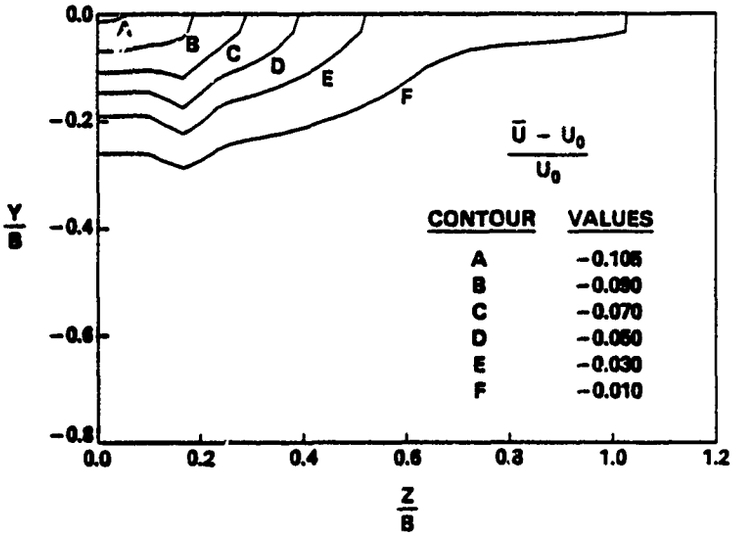

(a) Contours of mean streamwise velocity

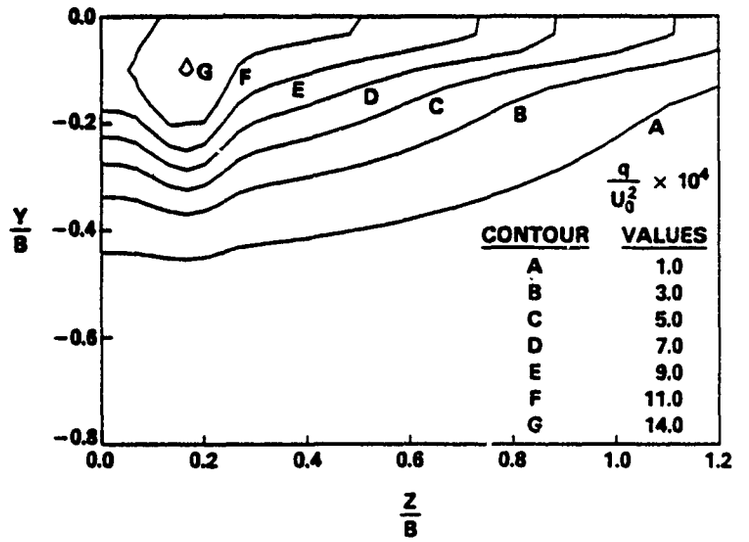

(b) Contours of turbulence kinetic energy

Fig. 9 — Distributions of Initial Profile Data — wake of hull, rudder and breaking bow wave

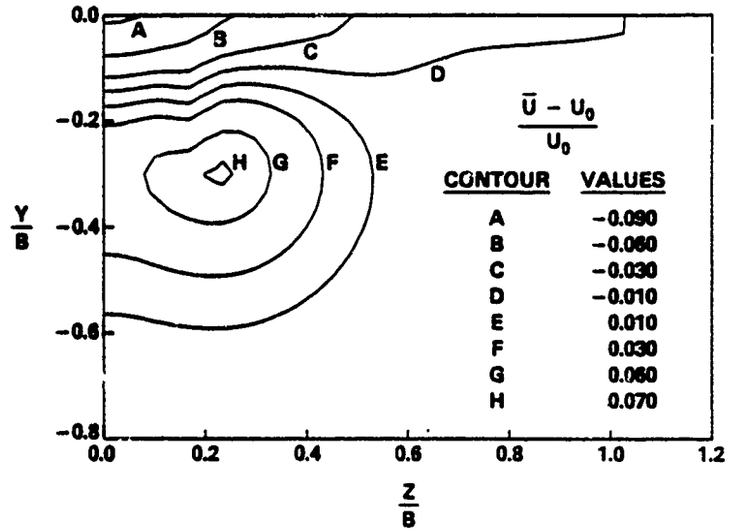

(a) Contours of mean streamwise velocity

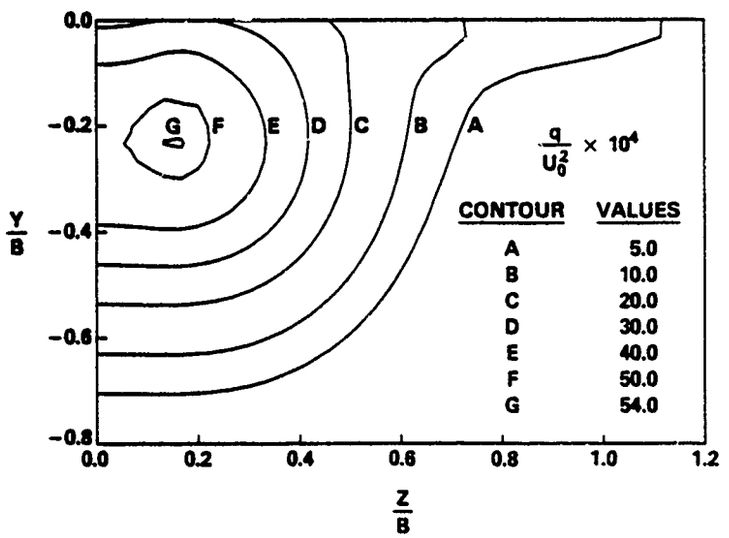

(b) Contours of turbulence kinetic energy

Fig. 10 — Distributions of Initial Profile Data — wake of hull, rudder, breaking bow wave and propeller

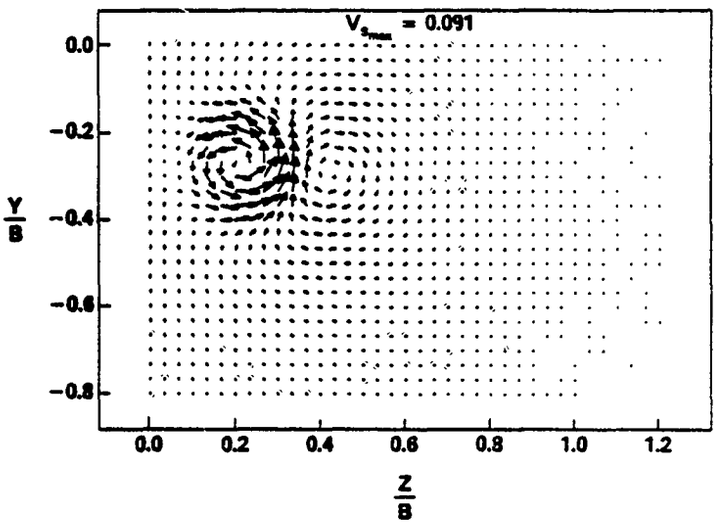

Fig. 11 — Distribution of Initial Profile Data — swirl velocity vectors — propeller and bilge vortex at 5% of Swanson value

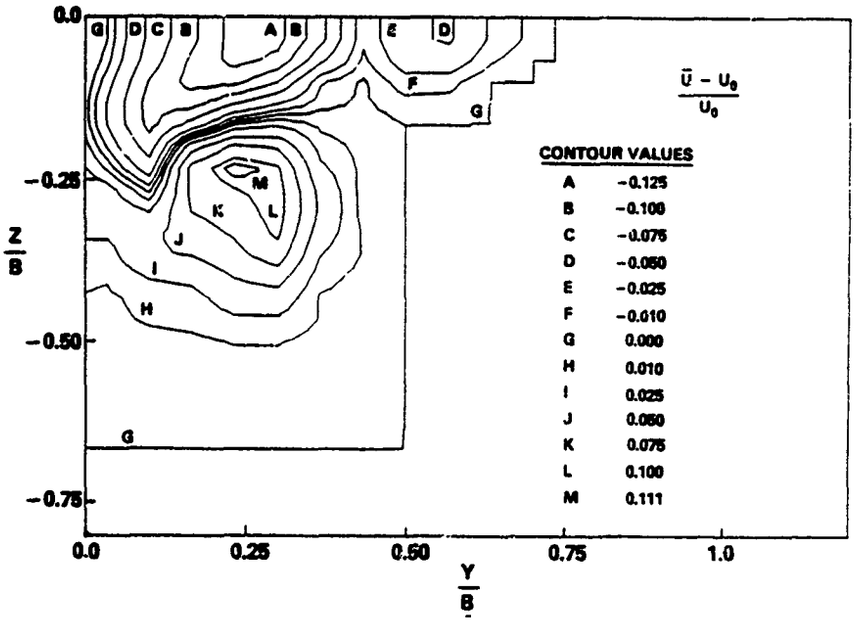

Fig. 12 — Mean streamwise velocity distribution based on experimental data

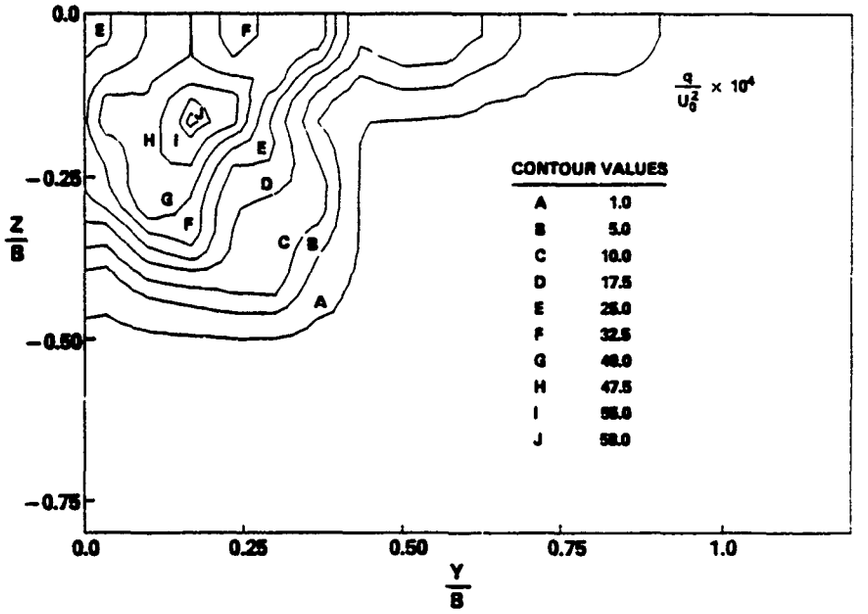

Fig. 13 — Turbulence kinetic energy distribution based on experimental data

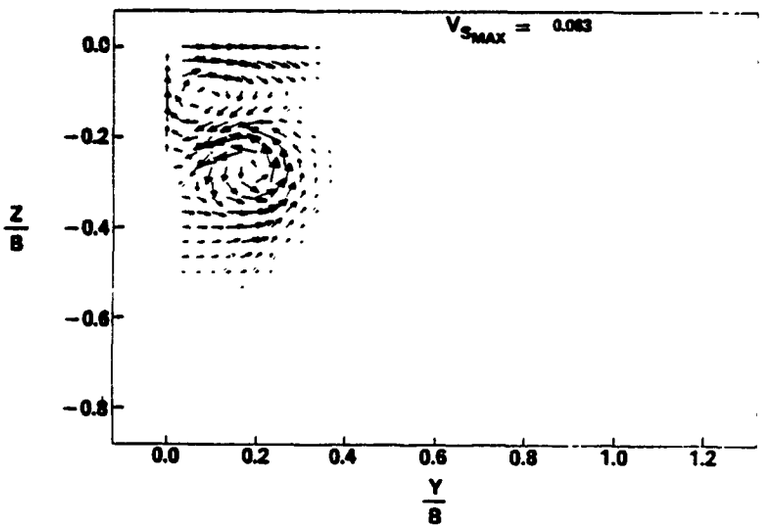

Fig. 14 — Swirl velocity vectors based on experimental data

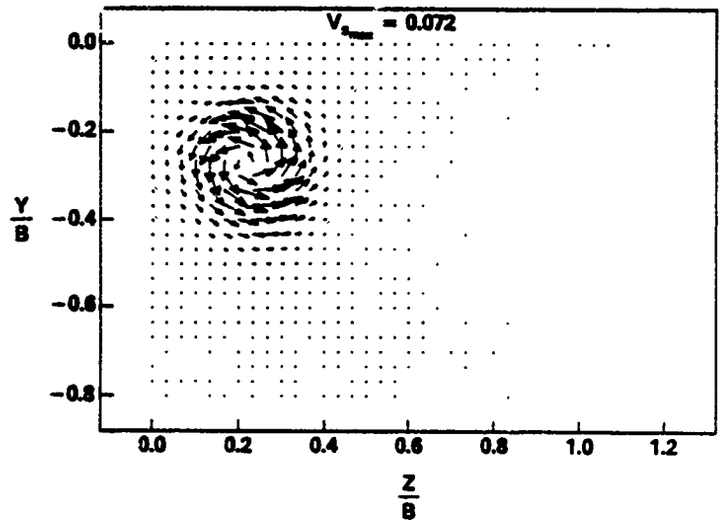

Fig. 15 — Propeller swirl velocity vectors after adjustment to approximately satisfy continuity